

# Neuro-network simulation of the dynamics of the Earth's ozone layer (neuro-network models)

I.Yu. Sakash, Yu.P. Lankin, V.B. Kashkin, M.N. Kolyada, and S.V. Smirnov

*Krasnoyarsk State Technical University  
Institute of Biophysics,  
Siberian Branch of the Russian Academy of Sciences, Krasnoyarsk*

Received September 17, 2001

Studying the ozone layer is an important part of investigation of the Earth's atmosphere because of the high significance of ozone for life and temperature conditions on our planet. The results concerning simulation of the ozone layer and the Antarctic ozone hole with neural networks using satellite data are presented.

Multidimensional, nonlinear, dynamic (non-equilibrium) atmospheric processes are known to be extremely complicated for applying analytical descriptions to them. Methods of numerical simulation often prove efficient in such cases. However, traditional simulation methods have some fundamental limitations. These have been revealed in Ref. 1, where the general abstract characteristic of the perturbation theory was obtained. It follows, from this characteristic, that *variation of the initial and/or boundary conditions in the process of verification of a model is insufficient for simulation (control) of complex systems and processes*. In Ref. 1 stochastization of any processes starting from the second approximation is proved analytically. This means that the correct operation with the atmospheric models considered is possible only within the first approximation. Adaptive systems and systems (in particular, neural networks with independent adaptation) developed for mapping the information organization of a brain and hierarchic, non-equilibrium natural systems are just the approach that allows one to hold within the framework of the first approximation.<sup>2</sup>

The efficiency of neural networks for solution of complicated nonlinear problems is justified theoretically in Ref. 3, where it is shown that it is possible to obtain arbitrarily accurate approximation of any continuous function of many variables using the standard (for neural networks) operations such as addition and multiplication by a number, superposition of functions, linear functions, as well as one arbitrary continuous linear function of one variable. This means that to obtain the needed result, the only required property of the neuron activation function is its nonlinearity [see Eq. (1)].

The use of neural networks (and, in a more general case, adaptive networks and systems) allows us to remove the most complicated part, namely, formalization of a problem and to construct the mathematical representation through learning of a neural network using experimental data. In many cases, this approach significantly speeds up and facilitates this stage of investigations.

It should be noted that construction of complicated, dynamic, hierarchic models is an extremely difficult problem when using traditional simulation methods. However, current methods of neuro-informatics allow us to overcome this barrier and to develop nonlinear integral adaptive models of high complexity taking into account numerous mutually related parameters. One of the advantages of such models is the possibility of evaluating the significance of input parameters for obtaining the expert judgments mentioned above. This circumstance yields new knowledge of the importance of different factors in the formation and following dynamics of the studied phenomena and processes. In addition to a more complete insight into the nature of an object under study, we get the possibility of efficiently simplifying models for saving computer resources and more rapid obtaining the simulated results and expert judgments.

Development of *the concept of self-adaptation networks and systems*<sup>2</sup> generalizing the capabilities of classic neural networks and having some non-traditional capabilities on construction of adaptive, dynamic systems with a search behavior allowed us to pass on to the study of new classes of models that caused serious problems in the past. In particular, the algorithms constructed according to its requirements<sup>4</sup> provide for processing of space-time patterns with a complex continuous structure. Self-adaptation neuro-networks<sup>4</sup> can reproduce various, in particular, hierarchic structures of systems with synchronous and asynchronous functioning, evolving at infinitely long periods, and form various types of learning estimates of constructed models, including distributed ones.<sup>5</sup> Thus, the use of self-adaptation neuro-networks gives a powerful apparatus for simulation and check of various hypotheses in atmospheric physics.

One of the simple versions of the neuro-network learning algorithm of the type considered looks like the following.<sup>4</sup>

Let neuron functioning in a neuro-network be described by the equation

$$\alpha_i = \arctan \rho_i, \quad \rho_i = \sum_j \alpha_j x_{ij} + A_i, \quad (1)$$

where  $A_i$  are external input signals;  $\alpha_j$  are input signals from other neurons;  $x_{ij}$  are weights of interneuron connections.

The goal function, which is used for evaluation of learning (adaptation) success, is specified as:

$$H = \frac{1}{2} \sum_i (\alpha_i - \alpha_i^*)^2, \quad (2)$$

where  $\alpha_i^*$  are the needed values of  $\alpha_i$ . Other possibilities obviously exist as well.

The process of random search yields a series of  $\{\rho_i\}$  values, which meet the condition of improvement of the estimating function. This is the time series  $\rho_t$ , whose behavior is to be predicted ( $\rho_t$  is the value of  $\rho_i$  at some time).

Let the time series generated by some model be  $\rho_t = \delta_t + \varepsilon_t$ , where  $\varepsilon_t$  is generated by a random non-autocorrelated process with the zero mathematical expectation and finite variance, and  $\delta_t$  can be generated either by a deterministic function or a random process, or by their combination.

The tendency of a dynamic series can be calculated and analyzed through exponential smoothing of the series. This process is based on calculation of exponential means. Exponential smoothing is described by the recursion formula  $S_t = v\rho_t + \beta S_{t-1}$ , where  $S_t$  is the exponential mean at the time  $t$ ;  $v$  is the smoothing parameter,  $v = \text{const}$ ,  $0 < v < 1$ ;  $\beta = 1 - v$ . Another way is the use of the time series  $\rho_t$ :

$$S_t = v \sum_{l=0}^{N-1} \beta^l \rho_{t-l} + \beta^N S_0, \quad (3)$$

where  $N$  is the number of terms in the series;  $S_0$  is the parameter characterizing the initial conditions for first application of the formula at  $t = 1$ . Since  $\beta < 1$ ,  $\beta^N \rightarrow 0$  at  $N \rightarrow \infty$ , and

$$v \sum_{l=0}^{N-1} \beta^l \rightarrow 1. \quad (4)$$

Then

$$S_t = v \sum_{l=0}^{\infty} \beta^l \rho_{t-l}. \quad (5)$$

Thus,  $S_t$  is the weighted sum of all terms in the series.

Let the series be generated by the model  $\rho_t = a_1 + \varepsilon_t$ , where  $a_1 = \text{const}$ ,  $\varepsilon_t$  is the random non-autocorrelated deviation or noise with the zero mean and the variance  $\sigma^2$ .

Apply the exponential smoothing procedure to it. Then

$$\begin{aligned} S_t &= v \sum_{l=0}^{\infty} \beta^l \rho_{t-l} = v \sum_{l=0}^{\infty} \beta^l (a_1 + \varepsilon_{t-l}) = \\ &= a_1 + v \sum_{l=0}^{\infty} \beta^l \varepsilon_{t-l}. \end{aligned} \quad (6)$$

Find the mathematical expectation  $M(S_t) = M(\rho_t) = a_1$  and variance

$$\begin{aligned} D(S_t) &= M[(S_t - a_1)^2] = M\left[\left(v \sum_{l=0}^{\infty} \beta^l \varepsilon_{t-l}\right)^2\right] = \\ &= v^2 \sum_{l=0}^{\infty} \beta^{2l} \sigma^2 = \frac{v}{2-v} \sigma^2. \end{aligned} \quad (7)$$

Since  $0 < v < 1$ ,  $D(S_t) < D(\rho_t) = \sigma^2$ . Thus, the exponential mean  $S_t$  has the same mathematical expectation as the series  $\rho$ , but its variance is smaller. At a high value of  $v$ , the variance of the exponential mean only slightly differs from the variance of the series  $\rho$ .

To apply the exponential mean to short-term prediction, we use the series generated by the model  $\rho_t = a_{1,t} + \varepsilon_t$ , where  $a_{1,t}$  is the mean level of the series variable in time;  $\varepsilon_t$  is the random non-autocorrelated deviation with zero mathematical expectation and the variance  $\sigma^2$ . The prediction model has the form  $\hat{\rho}_\tau(t) = \hat{a}_{1,t}$ , where  $\hat{\rho}_\tau(t)$  is the prediction obtained at the time  $t$  for  $\tau$  time units (steps) in advance;  $\hat{a}_{1,t}$  is the estimate of  $a_{1,t}$ . The exponential mean  $S_t$  serves an estimate for the model parameter  $a_{1,t}$ :  $\hat{a}_{1,t} = S_t$ . All the properties of the exponential mean are, at the same time, the properties of the prediction model. If  $S_{t-1}$  is the prediction for one step in advance, then  $(\rho_t - S_{t-1})$  is an error of this prediction, while the new prediction  $S_t$  follows from correcting the previous prediction with the made allowance for the error.

## Prediction of the annual mean total ozone content (TOC)

Based on the neuro-network models described, we have performed some studies aimed at the development of adaptive computer models of the ozone layer dynamics. At this stage of our investigation, our task was not a detailed reconstruction of the ozone fluctuations, since the emphasis was on testing the simulation apparatus and procedure with the allowance for features of the object under study. The task of the neural network was learning to catch the general regularities in the ozone variation with a preset resolution in space and time. The capability of a neural network to learn in the supervisor mode was used.

For predicting, we took the annual mean TOC in Arosa, Switzerland (9°40' E, 46°45' N). The corresponding data are plotted in Ref. 6.

Figure 1 depicts the annual mean TOC in Arosa. The neural network used for learning the period from 1929 to 1981. The prediction was made for the test period from 1982 to 1989. The learning sample involved 45 TOC values, and the test included 8 values. The model was developed based on the neural network consisting of seven neurons. The prediction quality turned out rather high. The correlation coefficient between the preset and predicted curves was  $R = 0.93$ .

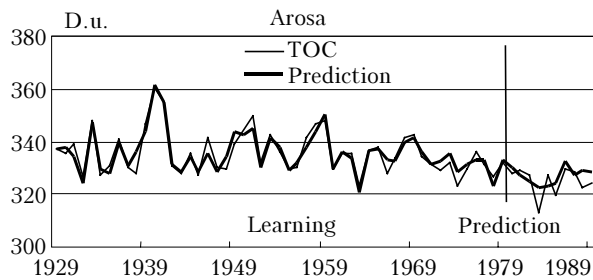


**Fig. 1.** Annual mean TOC for the period from 1982 to 1989 predicted based on the learning sample from 1929 to 1981.

In Fig. 1, the curve TOC shows real data on measurement of ozone content in stratosphere. The curve “prediction” shows results of neuro-network model operation: to the left from vertical dashed line there is learning of neuro-network, to the right – TOC prediction by neuro-network.

The results obtained showed the possibility of constructing local prediction models based on neural networks under conditions of deficient information on the atmospheric processes.

As can be seen from Fig. 1, the task formulated for the experiments described has been successfully achieved. Further improvement of the prediction calls for additional information to be introduced into the model. Presumably, consideration of the solar activity, anthropogenic factor, and atmospheric turbulence, in particular, circumpolar vortices, can markedly improve the accuracy of prediction.

## Study of the Antarctic ozone hole

The phenomenon of the ozone hole consists in the steady TOC decrease in the near-polar zone in September–October, as well as later spring peaking, whose intensity, as well as TOC in other months of the 1980s, only slightly differs from the mean “climatic” values of the previous years. There exist two hypotheses of the ozone hole formation: anthropogenic photochemical and meteorological.

A circumpolar vortex that forms every year after the March equinox signalizes the beginning of Antarctic winter. It is a circulating mass of very cold stagnant air confined within a ring of western winds. This extreme weather phenomenon arises because of the unique geographic conditions of the Antarctic surrounded by oceans and devoid of massifs, which could create a more complex air circulation system. The vortex destructs only when the stratospheric temperature increases, that is, roughly a month before the equinox.

Thus, circulation vortex exists during 8–9 months in a year, since the end of March till the beginning of December. In summer (in December) at the altitudes corresponding to the pressure of 100 and 50 hPa the temperature in the Antarctic is roughly 40°C higher than in winter. Moreover, the temperature gradient along a meridian alternates: it becomes opposite to that in winter. This means that the winds alternate the direction from western to eastern, that

is, the circumpolar vortex in summer is eastern unlike the western one in winter. However, there is one more very important principle difference between the winter and summer vortices. It is that the summer eastern vortex is weak, and therefore it does not prevent from air masses coming from the mid-latitudes to the pole.<sup>7</sup>

The relation of the ozone hole to the circumpolar vortex was studied by many scientists from different countries both experimentally and theoretically with the use of various models. The idea of this relation is obvious and very simple: the presence of a vortex (whirlpool) around the pole prevents from coming of ozone-rich air from the mid-latitudes into the vortex. Thus, on the one hand, ozone is not produced under the exposure to the solar radiation during the long polar night, and, on the other hand, it is destructed due to the presence of chlorine components (admixture). Measurements showed that in the areas with the decreased ozone content, the amount of active ClO is 10–500 times higher than under normal conditions (with no ozone holes) and as compared to the mid-latitudes. Likely, just ClO is the main cause of the ozone hole, and the presence of ClO in the stratosphere is the result of the human activity. The circumpolar vortex only forms the conditions favoring ozone depletion, namely, the presence of small particles of polar stratospheric clouds. Formation of stratospheric clouds depends, first, on the stratospheric temperature at the given place. They are formed in winter, when the stratospheric air over the Antarctic is very cold because of the absence of solar irradiation.

When the spring comes, the sun rises higher above the horizon, and the Antarctic stratosphere warms up. Under the effect of heat and sunlight, polar clouds disappear and active nitrogen compounds released at melting and evaporation of rest crystals intervene in the atmospheric chemistry. In addition, ozone is transferred into the ozone hole from the near-polar latitudes.

Formation of the ozone hole is usually associated with the Antarctic circumpolar vortex – a steady cyclonic circulation in the lower stratosphere, which is over the polar region for the whole Antarctic winter and spring.

As known, air inside this vortex moves, in the first approximation, along closed trajectories around the South Pole.

More detailed investigation of air mass motion in the atmosphere is presented in Ref. 8, and ozone serves an indicator, as if ozone formations are natural sounding balloons. If we compare TOC maps for several days, then we can determine the speed and direction of motion of the ozone layer and the stratosphere as a whole at the altitudes of the maximum ozone content (18–25 km).

Figure 2 depicts the TOC field in the Southern Hemisphere for September 29–30 of 2000 drawn based on EP/TOMS satellite data. The field looks like as a “billow” with high TOC (up to 470 D.u.) about 7000 km in diameter that surrounds the zone with low TOC (ozone hole).

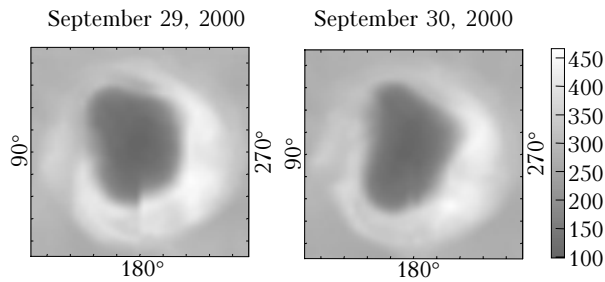


Fig. 2. Ozone layer in the Southern Hemisphere in late September of 2000.

It is seen from Fig. 2 that for the day the ring turned through some angle in the eastern direction and extended a little bit.

To determine the quantitative characteristics of the ozone motion in the stratosphere, a Dynamic suit of applied programs has been developed. It converts the data from the dat format into the form used in tabular processors. The main module calculates the speed and direction of motion of ozone masses using a correction-extreme algorithm<sup>8</sup>: the correlation coefficient between the TOC field for one day and that shifted and turned by some angle for the previous day is calculated. The highest value of the sampled correlation coefficient, which achieves sometimes 0.95–0.98, corresponds to the diurnally mean shift and turn of the field. The TOC field can be divided into rings centered at the South Pole, and the speed and direction of motion in each of these rings can be determined.

Figure 3 depicts the latitude dependence of the mean speed of air mass (along with ozone) motion obtained from comparison of the TOC fields for September 4 and 5 of 2000, in the period of ozone hole formation; every field was divided into 5°-wide rings. The latitudinal TOC distribution averaged over the Southern Hemisphere for September 5 is depicted in Fig. 3 as well.

As follows from Fig. 3, the maximum of the speed along a parallel (speed of circulation) coincides with the mean TOC maximum at 40–45°S. In Figs. 3 and 4, the positive values of the meridional speed correspond to the motion from the equator, while the negative ones stand for the motion toward the equator. Analysis showed that inside the ozone hole in the period of its formation at the latitudes from 70 to 85° the stratospheric air masses, first, circulate with significant speed (up to 24 deg/day) and, second, move toward the equator, that is, toward the billow. Thus, the ozone masses leave the region near the South Pole, in which the ozone concentration decreases. By the end of the period of ozone hole formation, the speed of circulation decreases. In year 2000 the deepest ozone hole was observed on September 29–30. In this period, the speed of circulation inside the hole vanished (Fig. 4), and in October it did not exceed 5 deg/day. Starting from September 30 the steady motion of the ozone masses toward the South Pole was observed inside the billow.

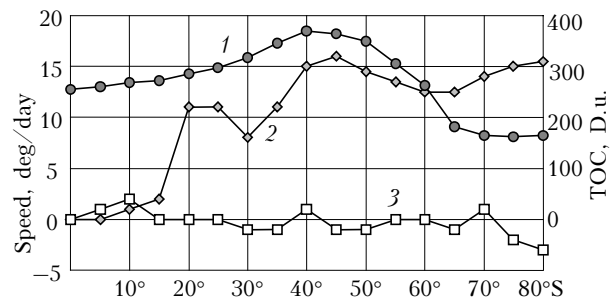


Fig. 3. Latitude dependence of the ozone mass motion on September 4–5: TOC latitudinal distribution (1), speed along a parallel (2), speed along a meridian (3).

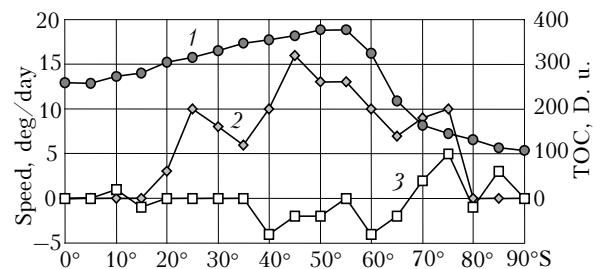


Fig. 4. Latitude dependence of the ozone mass motion on September 29–30: TOC latitudinal distribution (1), speed along a parallel (2), speed along a meridian (3).

Based on the above-said, we can propose one more additional mechanism of formation and destruction of the ozone hole. At high speed of air mass circulation inside the ozone hole, a significant centrifugal force arises, which “presses” ozone to the billow (centrifugal effect), and therefore in the period of the ozone hole formation a flow directed from the pole toward the equator appears inside the billow. In the period of the ozone hole destruction, the speed of circulation decreases drastically, and the hole is filled with ozone. These processes are natural and not connected with the effect of ozone-destructive substances of anthropogenic origin.

## References

1. V.O. Bytev, in: *Symmetry and Differential Equations. Proc. Int. Conf.* (ICM SB RAS, Krasnoyarsk, 2000), pp. 59–62.
2. J.P. Lankin, *Proc. SPIE* **4678**, 669–680 (2002).
3. A.N. Gorban', *Sib. Zh. Vychisl. Matem.*, No. 1, 11–24 (1998).
4. T.F. Baskanova and Yu.P. Lankin, *Izv. Vyssh. Uchebn. Zaved., Ser. Fizika*, No. 6, 47–51 (2000).
5. Yu.P. Lankin, in: *Proc. IX Int. Symp. on Reconstruction of Homeostasis*, (KSC SB RAS, Krasnoyarsk, 1998), Vol. 1, pp. 281–287.
6. E.L. Aleksandrov, Yu.A. Izrael, I.L. Karol, and A.H. Khrgian, *Ozone Shield of the Earth and Its Dynamics* (Gidrometeoizdat, St. Petersburg, 1992), 287 pp.
7. Yu.V. Mizum and Yu.G. Mizun, *Ozone Holes and Death of Mankind?* (Veche, Moscow, 1998).
8. N.N. Beloglazov and V.P. Tarasenko, *Correlation-Extreme Systems* (Sov. Radio, Moscow, 1974), 392 pp.